nature catalysis

SUPPLEMENTARY INFORMATION

https://doi.org/10.1038/s41929-019-0419-z

In the format provided by the authors and unedited.

Photocatalytic uphill conversion of natural gas beyond the limitation of thermal reaction systems

Shusaku Shoji[1], Xiaobo Peng[2], Akira Yamaguchi[1], Ryo Watanabe[3], Choji Fukuhara[3], Yohei Cho[1], Tomokazu Yamamoto[4], Syo Matsumura[4], Min-Wen Yu[5], Satoshi Ishii[2], Takeshi Fujita[6]*, Hideki Abe[2]* and Masahiro Miyauchi[1]*

[1]Tokyo Institute of Technology, Tokyo, Japan. [2]National Institute for Materials Science, Tsukuba, Japan. [3]Shizuoka University, Hamamatsu, Japan. [4]Kyushu University, Fukuoka, Japan. [5]National Chiao Tung University, Tainan, Taiwan. [6]Kochi University of Technology, Kami, Japan.
*e-mail: fujita.takeshi@kochi-tech.ac.jp; ABE.Hideki@nims.go.jp; mmiyauchi@ceram.titech.ac.jp

Supplementary Information

Photocatalytic uphill conversion of natural gas beyond the limitation of thermal reaction systems

Authors: Shusaku Shoji[1], Xiaobo Peng[2], Akira Yamaguchi[1], Ryo Watanabe[3], Choji Fukuhara[3], Yohei Cho[1], Tomokazu Yamamoto[4], Syo Matsumura[4], Min-Wen Yu[5], Satoshi Ishii[2], Takeshi Fujita[6]*, Hideki Abe[2]* and Masahiro Miyauchi[1]*

Affiliations:

1 Tokyo Institute of Technology, 2-12-1 Ookayama, Meguro-ku, Tokyo152-8552, Japan

2 National Institute for Materials Science, Namiki 1-1, Tsukuba, Ibaraki 305-0044, Japan

3 Shizuoka University, Johoku3-5-1, Naka-ku, Hamamatsu City, Shizuoka, Japan

4 Kyushu University, 744 Motooka, Nishi-ku, Fukuoka 819-0395, Japan

5 National Chiao Tung University, 301 Gaofa 3rd Road, Tainan 711, Taiwan

6 Kochi University of Technology, 185 Miyanokuchi, Tosayamada, Kami City, Kochi 782-8502

*E-mail: mmiyauchi@ceram.titech.ac.jp

Supplementary methods

Calculation methods

The thermodynamic limit of DRM was calculated by the calculation software of NASA-CEA[1]
(S. Gordon and B. J. McBride, "Computer Program for Calculation of Complex Chemical Equilibrium Compositions and Applications," NASA Reference Publication 1311 (1996).)

Supplementary equations

The conversion, quantum efficiency (QE) and turn over number were calculated as below.

Supplementary equation 1

$$\text{Conversion of } CH_4\ (\%) = \frac{CH_4\ input - CH_4\ output}{CH_4\ input} \times 100$$

Supplementary equation 2

$$\text{Conversion of } CO_2\ (\%) = \frac{CO_2\ input - CO_2\ output}{CO_2\ input} \times 100$$

Supplementary equation 3

$$\text{Quantum efficiency}\ (\%) = \frac{Electrons\ number\ for\ product}{Absorbed\ photon\ number} \times 100$$

Supplementary equation 4

$$\text{Turn over number} = \frac{Product\ amount\ (mol)}{Rh\ amount\ (mol)}$$

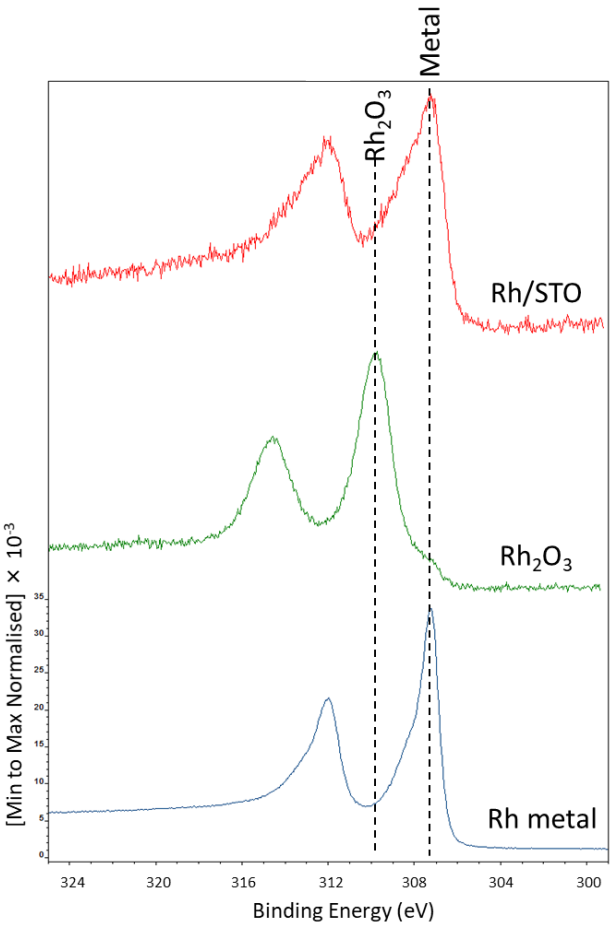

Supplementary Figure 1. XPS of Rh metal (bottom, blue line), Rh_2O_3/STO (middle, green line), and Rh/STO (top, red line), respectively. The dashed lines indicate the representative peaks of Rh_2O_3 and Rh metal.

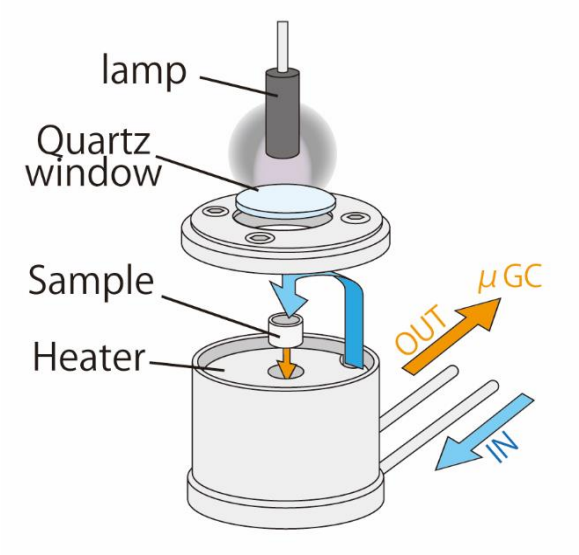

Supplementary Figure 2. Schematic illustration of the DRM reactor.

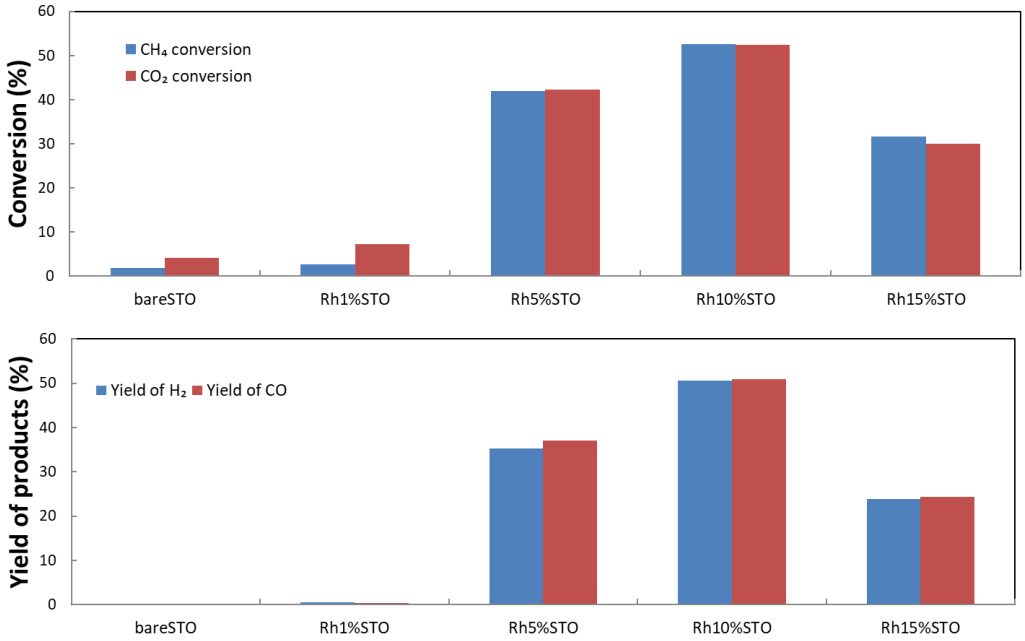

Supplementary Figure 3. DRM performance of Rh/STO samples with different Rh loading amount under UV irradiation.

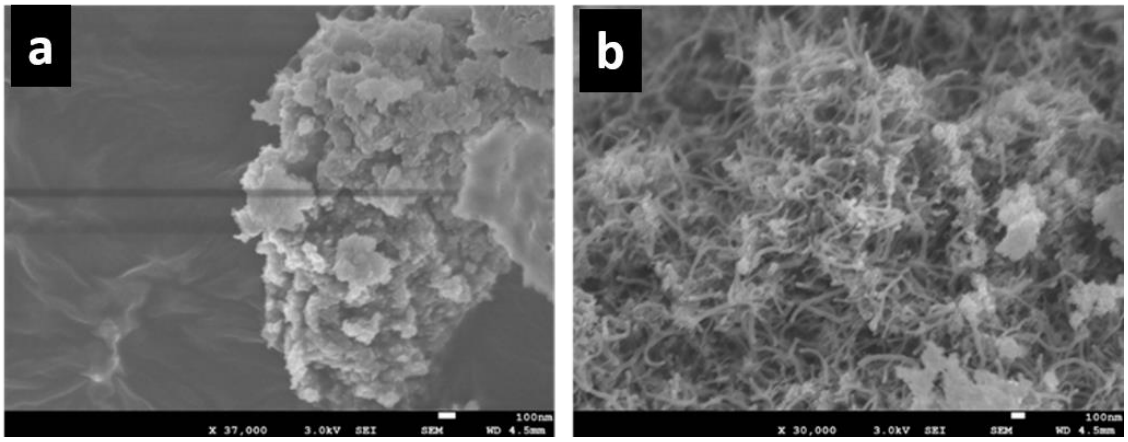

Supplementary Figure 4. SEM images of Ni/Al_2O_3 before (a) and after DRM (b) at 500 °C for 5 hours.

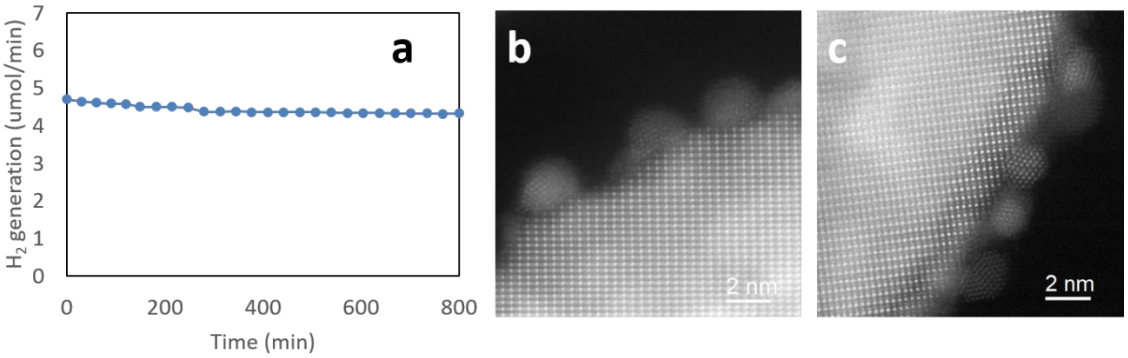

Supplementary Figure 5. Long-term stability for the H_2 production over the Rh/STO (a). HAADF-STEM images of Rh/STO before DRM (b) and 10 hours after DRM (c).

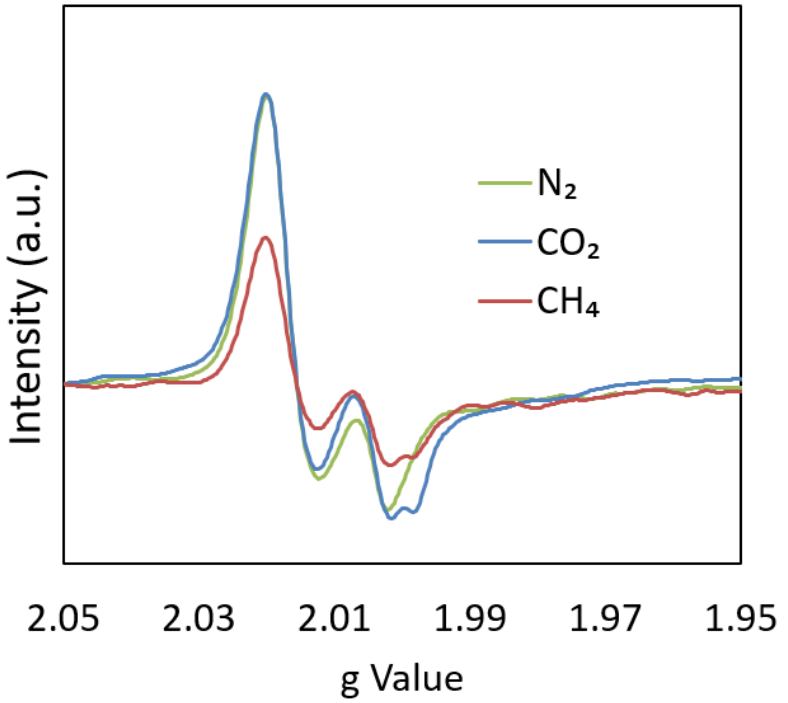

Supplementary Figure 6. Electron spin resonance (ESR) spectroscopy of Rh/STO under light irradiation in N_2 (green line), CO_2 (blue line), and CH_4 atmosphere (red line), respectively.

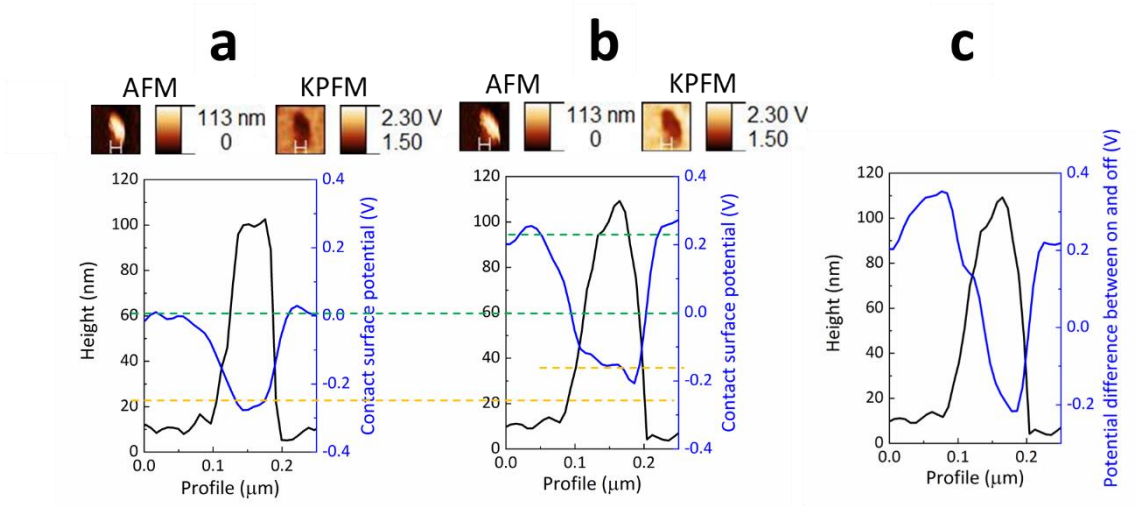

Supplementary Figure 7. Kelvin probe force microscope (KPFM) analysis on the Rh loaded STO single crystal (110), (a) before UV light irradiation, (b) during UV light irradiation, and (c) potential difference between light-on and light-off conditions, respectively. The cross sectional profiles of the atomic force microscope (AFM) and the KPFM analyses were taken in horizontal direction. The sample was prepared by the same manner with powder preparation of Rh/STO. The scale bars on the AFM images show 60 nm. The contact surface potential of the STO before UV light irradiation is set to 0 V.

According to the subtract potential profile between light-on and light-off condition (panel c), the Fermi level upshift of STO by light irradiation was more obvious than that of Rh particle, since the electron transition through band gap excitation was happened in STO. Consequently, the electrons in STO can transfer to Rh following their gap of Fermi levels. Indeed, the Fermi level upshift of Rh particle was also seen (dashed yellow lines). These results strongly imply the electron transport between semiconductor and metal interface.

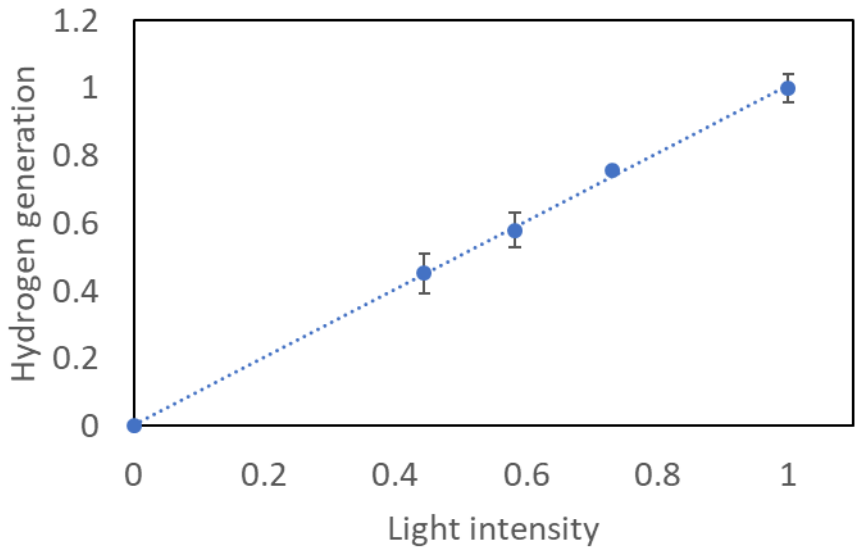

Supplementary Figure 8. Light intensity dependence on hydrogen generation rate of Rh/STO. To simplify the figure, hydrogen generation rate in the vertical axis is normalized. The error bars represent the standard deviation by taking data more than twice.

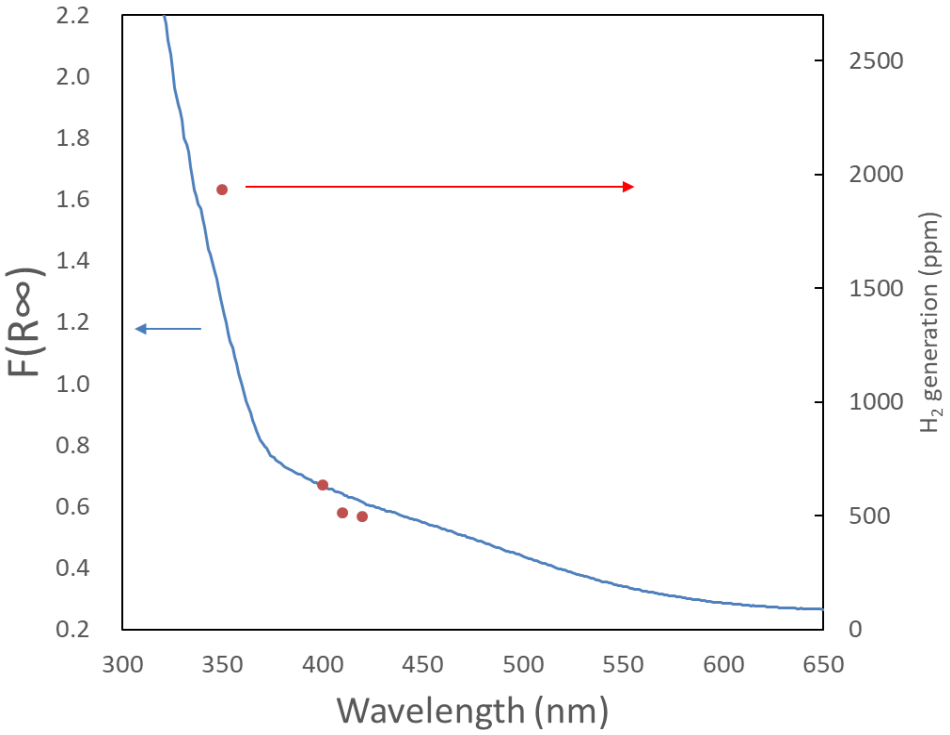

Supplementary Figure 9. UV-vis spectrum of Rh-STO (F: optical absorption drawn by blue line) and action spectrum of DRM activity (red circles). The action spectrum shows that the reaction was boosted below the wavelength of 380 nm, which corresponds to the band gap energy of STO (3.2 eV).

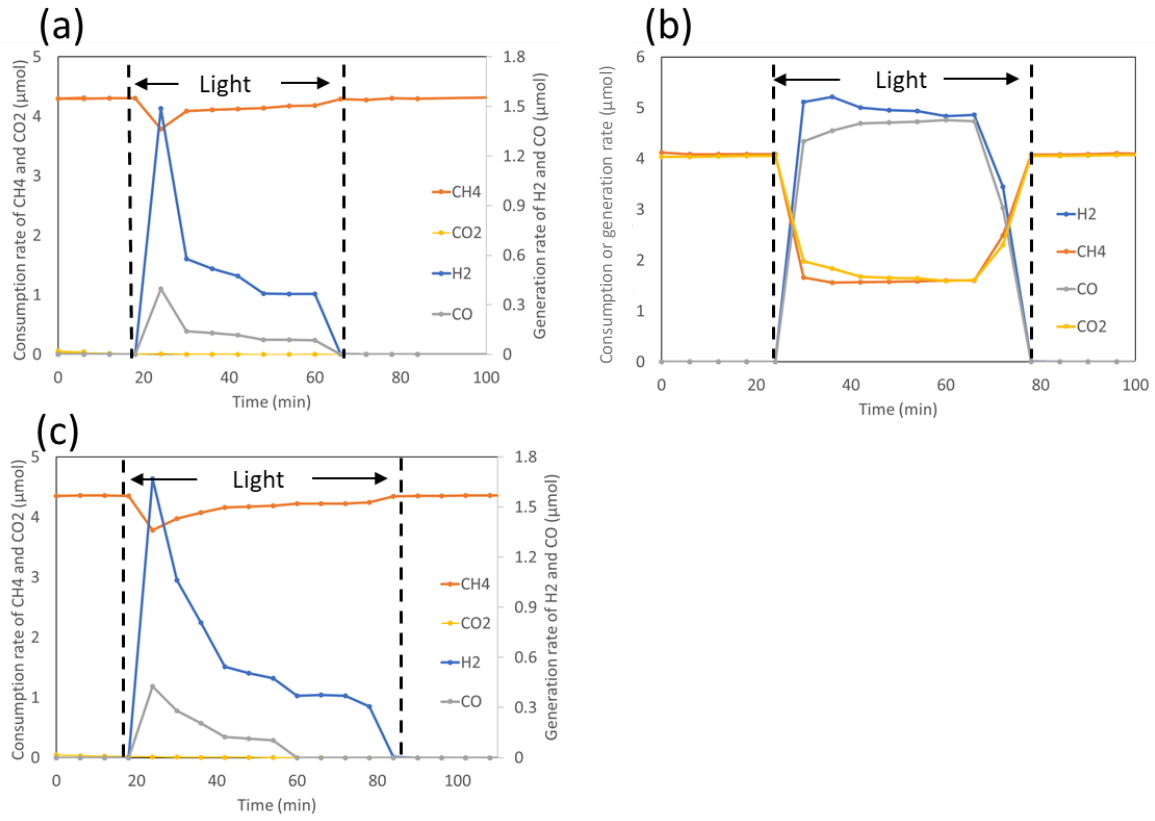

Supplementary Figure 10. Catalytic activity of Rh/STO in the presence of sole CH_4 (a), CO_2 and CH_4 mixture (b), and sole CH_4 condition again (c). For each panel prior to reaction, the gases were flowed into reactor and the reactor was heated at 150 °C to remove surface absorbed molecules. The test was subsequently conducted from (a) to (c) in order.